

The N-terminus of a *Fusarium graminearum*-secreted protein enhances broad-spectrum disease resistance in plants

Qiang Xu^{1,2}  | Su Hu^{1,2} | Minxia Jin^{1,2} | Yangjie Xu^{1,2} | Qiantao Jiang^{1,2} | Jian Ma^{1,2} | Yazhou Zhang^{1,2} | Pengfei Qi^{1,2} | Guoyue Chen^{1,2} | Yunfeng Jiang^{1,2} | Youliang Zheng^{1,2}  | Yuming Wei^{1,2}

¹State Key Laboratory of Crop Gene Exploration and Utilization in Southwest China, Sichuan Agricultural University, Chengdu, China

²Triticeae Research Institute, Sichuan Agricultural University, Chengdu, China

Correspondence

Yuming Wei, State Key Laboratory of Crop Gene Exploration and Utilization in Southwest China, Sichuan Agricultural University, Chengdu, Sichuan, China. Email: ymwei@sicau.edu.cn

Funding information

Applied Basic Research Programs of Science and Technology Department of Sichuan Province, China, Grant/Award Number: 2021YJ0298; National Natural Science Foundation of China, Grant/Award Number: 32102229; Sichuan Science and Technology Program, China, Grant/Award Number: 2022ZDZX0014

Abstract

Fusarium head blight is a destructive disease caused by *Fusarium* species. Little is known about the pathogenic molecular weapons of *Fusarium graminearum*. The gene encoding a small secreted protein, Fg02685, in *F. graminearum* was found to be up-regulated during wheat head infection. Knockout mutation of Fg02685 reduced the growth and development of *Fusarium* in wheat spikes. Transient expression of Fg02685 or recombinant protein led to plant cell death in a BAK1- and SOBIR1-independent system. Fg02685 was found to trigger plant basal immunity by increasing the deposition of callose, the accumulation of reactive oxygen species (ROS), and the expression of defence-related genes. The Fg02685 signal peptide was required for the plant's apoplast accumulation and induces cell death, indicating Fg02685 is a novel conserved pathogen-associated molecular pattern. Moreover, its homologues are widely distributed in oomycetes and fungal pathogens and induced cell death in tobacco. The conserved α -helical motif at the N-terminus was necessary for the induction of cell death. Moreover, a 32-amino-acid peptide, Fg02685 N-terminus peptide 32 (FgNP32), was essential for the induction of oxidative burst, callose deposition, and mitogen-activated protein kinase signal activation in plants. Prolonged exposure to FgNP32 enhanced the plant's resistance to *Fusarium* and *Phytophthora*. This study provides new approaches for an environment-friendly control strategy for crop diseases by applying plant immune inducers to strengthen broad-spectrum disease resistance in crops.

KEYWORDS

cell death, filamentous fungi, *Fusarium graminearum*, pathogen-associated molecular patterns (PAMPs), plant immunity

Qiang Xu and Su Hu contributed equally to this work.

This is an open access article under the terms of the [Creative Commons Attribution-NonCommercial-NoDerivs](https://creativecommons.org/licenses/by-nc-nd/4.0/) License, which permits use and distribution in any medium, provided the original work is properly cited, the use is non-commercial and no modifications or adaptations are made.

© 2022 The Authors. *Molecular Plant Pathology* published by British Society for Plant Pathology and John Wiley & Sons Ltd.

1 | INTRODUCTION

The complex multilayers of plant immunity are challenged by natural co-evolution among pathogens. Plant cuticles and cell walls are two physical barriers to protect plants from pathogen infection. In addition, pattern recognition receptors present on the plant cytomembrane can recognize the conserved structures of pathogens, thereby stimulating a basal defence response (Goldman & Vicencio, 2012; Xu, Wang, et al., 2020b). Chitin oligomers and bacterial flagellin act as pathogen-associated molecular patterns (PAMPs) or microbe-associated molecular patterns (MAMPs), leading to the accumulation of reactive oxygen species (ROS), activation of defence-related genes, and augmented callose deposition on the plant cell wall, which are collectively called PAMP- or MAMP-triggered plant immunity (PTI) (Jones & Dangl, 2006; Ngou et al., 2022). Plants secrete antibacterial metabolites (phenols and alkaloids) and enzymes (hydrolases, chitinases, and proteases) to suppress the invading pathogens (Deising et al., 1995; Piasecka et al., 2015). A range of plant responses can severely hinder the development of pathogens in plant tissues during an infection.

PAMPs or MAMPs are evolutionarily conserved molecules widely found across bacteria, oomycetes, and fungi that play an essential role in plant-pathogen interactions. PAMPs include the intrinsic cell wall components, such as chitin, lipopolysaccharides, peptidoglycans, and glucans, and proteinaceous PAMPs, such as EF-Tu, flagellin, and cold-shock proteins from bacteria. For example, the 22-amino-acid peptide flg22 from bacterial flagellin is a classical PAMP and is sensed by flagellin-sensing 2 (FLS2) to stimulate cellular responses such as an oxidative burst and the transcriptional induction of downstream genes (Chinchilla et al., 2007; Denoux et al., 2008). Translation initiation factor 1 (IF1) isolated from *Ralstonia solanacearum* was recently demonstrated to bind to an RLP32 receptor, which recognizes the tertiary fold features of IF1 and induces PTI in *Arabidopsis thaliana* (Fan et al., 2022). The Pep-13, INF1, and XEG1 proteins of tobacco and potato oomycetes activate plant defence reactions (Brunner et al., 2002; Kamoun et al., 1998). XEG1, a glycoside hydrolase 12, degrades plant cell walls and contributes to *Phytophthora sojae* virulence. The paralogous PsXEG1-like protein PsXLP1 competitively binds to GmGIP1, protecting PsXEG1 from host inhibitors (Ma et al., 2017). However, compared to other pathogens, few proteinaceous PAMPs have been identified in filamentous fungi, like the first reported necrosis-inducing protein from *Fusarium oxysporum* (Bailey, 1995). Thus, necrosis-inducing proteins have mainly been found in filamentous fungi, oomycetes, and bacteria (Chen et al., 2018; Seidl & Ackerveken, 2019). However, knowledge of the mechanisms of PAMPs in filamentous pathogens is limited.

Fusarium graminearum is a pathogen mostly affecting the wheat and barley, forming complex appressoria and infection cushions before penetration (Boenisch & Schäfer, 2011). During the *F. graminearum*-wheat interaction, the release of the trichothecene mycotoxin deoxynivalenol from *F. graminearum* into the wheat head acts as a phytotoxin and virulence factor for the establishment

of hyphal infection (Audenaert et al., 2014). Deoxynivalenol acts as an inhibitor of protein synthesis, causing food safety risks and health hazards to animals and humans (Van De Walle et al., 2010). Recently, virulence factors including the *fg3_54* gene cluster and FgNahG have been isolated and identified from different infection stages (Qi et al., 2019). The nonribosomal octapeptide fusaoctatin A, encoded by *fg3_54*, is crucial for cell-to-cell hyphal invasion by *F. graminearum* in wheat (Jia et al., 2019). However, in the case of *F. graminearum*, the secreted proteins that directly interfere with host basal defence responses remain under investigation. The secreted protein FGL1 was found to cause release of polyunsaturated fatty acids, thereby inhibiting the deposition of plant callose in wheat spikes (Voigt et al., 2005). The secreted protein OSP24 was found to compete with the TaFROG protein for binding with the TaSnRK1 α kinase, thus regulating basal plant defence against virulent pathogens (Jiang et al., 2020).

This study characterized one putative MAMP, Fg02685, that induces cell death in the plant apoplast region in a BAK1- and SOBIR1-independent system to better understand the role of secreted proteins in *F. graminearum* pathogenesis. Fg02685 knockdown reduced fungal growth and disease development in infected wheat heads. Fg02685 homologues were widely distributed in oomycete and fungal pathogens, triggering programmed cell death in plants. Interestingly, a 32-amino-acid peptide including the conserved α -helix structure at the N-terminus of Fg02685, FgNP32, was found to activate the plant PTI response, including callose deposition, mitogen-activated protein kinase (MAPK) signal activation, oxidative burst, and the expression of defence-related genes. As a plant immune inducer, FgNP32 enhanced disease resistance against oomycetes and filamentous fungal pathogens in tobacco, soybean, and wheat.

2 | RESULTS

2.1 | Identification of apoplastic proteins secreted by *F. graminearum*

Several previous studies have identified 68 secreted proteins in the secretome of *F. graminearum* using liquid chromatography-mass spectrometry (LC-MS/MS) (Yang et al., 2021). After the removal of secreted proteins containing transmembrane and conserved domains (Sperschneider et al., 2018; Xu, Tang, et al., 2020a), 12 candidate proteins were identified: six apoplastic and six nonapoplastic, based on their localization in the plant apoplast (ApoplastP; Table S1). To further investigate the function of the apoplastic secreted proteins, these proteins were transiently expressed to examine the induction or suppression of plant cell death using the potato virus X (PVX) system in *Nicotiana benthamiana*. Five of the six apoplastic secreted proteins neither induced cell death in plants nor abolished the function of Bax, exerting the same effects as the negative control green fluorescent protein (GFP) (Figure S1).

However, one apoplastic secreted protein, Fg02685, induced plant cell death (Figure 1a). Trypan blue staining confirmed that

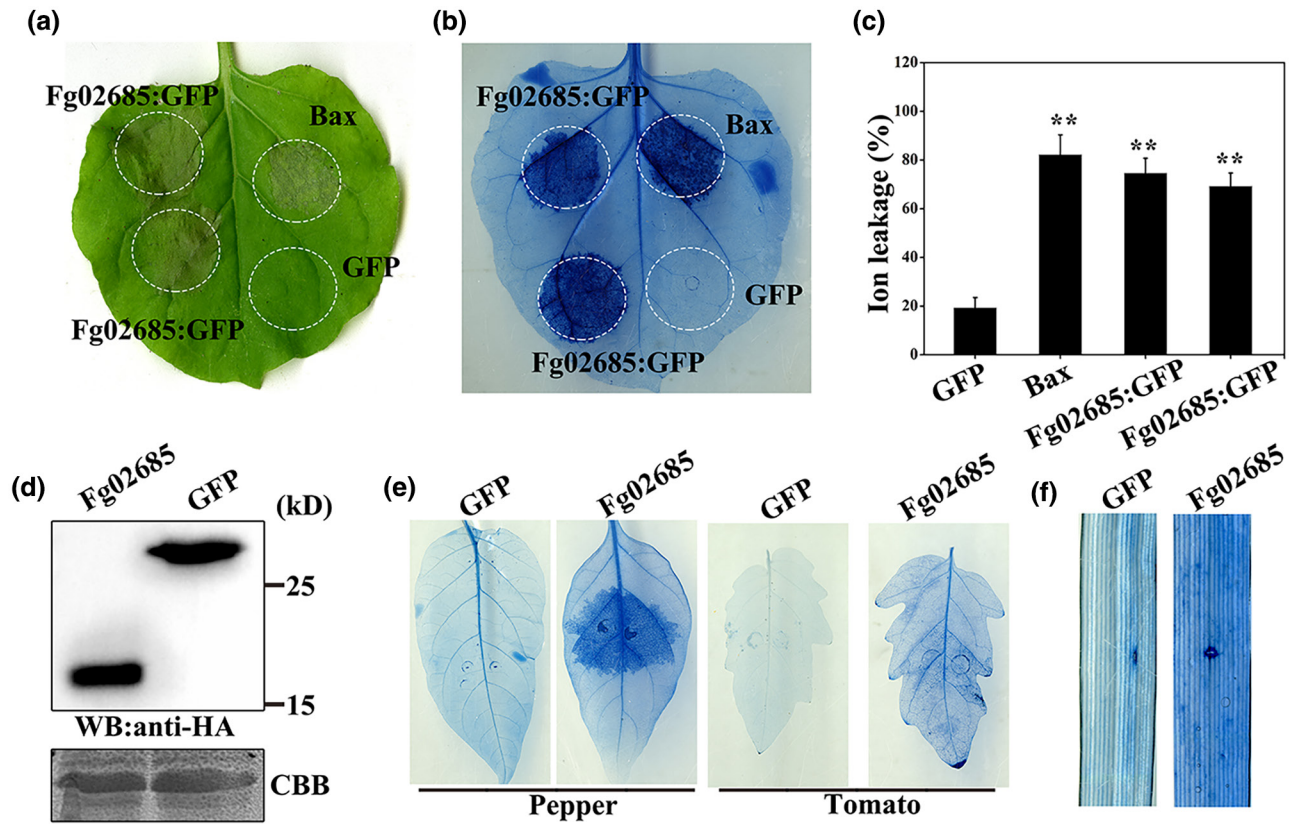


FIGURE 1 Induction of cell death by Fg02685 in multiple plant species. (a) Induction of cell death in *Nicotiana benthamiana* leaves. Fg02685 was transiently expressed in *N. benthamiana* leaves by the *Agrobacterium* system carrying PVX:GFP, PVX:Bax, or PVX:Fg02685. (b) The same leaf of the same set of *N. benthamiana* leaves as in Figure 1a was stained with trypan blue solution to visualize cell death symptoms. (c) Detection of electrolyte leakage in the tobacco leaves transiently expressing Fg02685 at 3 days postinoculation (dpi). The mean and standard deviation were calculated with data from three independent replicates. Asterisks indicate significant differences based on an unpaired two-tailed Student's *t* test (** $p < 0.01$). (d) The Fg02685:HA and GFP:HA proteins in the same leaf as in Figure 1a were detected by western blot with an anti-HA antibody. Coomassie brilliant blue (CBB) staining shows equal loading. (e) Cell death response in tomato and pepper leaves treated by the *Agrobacterium* system. (f) Induction of cell death was detected in the second wheat leaves with 1 μ M purified Fg02685 recombinant protein or GFP control. Phenotypes were photographed at 5 dpi.

macroscopic cell death was observed in the zone with Fg02685 infiltration (Figure 1b). Compared with the GFP zone, a significant change in the electrolyte leakage was observed in the region infiltrated with Fg02685 or with Bax (Figure 1c). This is consistent with the plant cell death phenotype in *N. benthamiana*. Western blot analysis with an anti-HA antibody confirmed the expression of Fg02685 in vivo (Figure 1d). A Fg02685:His fusion protein was expressed and purified from *Escherichia coli* to exclude the potential influence of the PVX system on Fg02685 production (Figure S2a). The ability of Fg02685 to induce cell death in *N. benthamiana* leaves was also examined by infiltrating the recombinant protein at concentrations varying from 10 to 1000 nM. The half maximal effective concentration (EC_{50}) was 35.68 nM and the degree of necrosis increased with the increase of Fg02685:His protein concentration (Figure S2b). Fg02685 was transiently expressed in tomato (*Solanum lycopersicum*) and pepper (*Capsicum annuum*) leaves to further test the specificity of the Fg02685-induced cell death. The infiltration result indicated that Fg02685 retained the ability to induce cell death in tomato, pepper, and wheat leaves (Figure 1e,f). Together, these results showed that Fg02685 could induce cell death in at least three plant species.

2.2 | The Fg02685 signal peptide is essential for cell death induction

The Fg02685 signal peptide was tested using an invertase enzyme to examine its function for secretion in yeast (Jacobs et al., 1997). The signal peptide was inserted into the pSuc2t7M13ori vector, which was transformed into the YTK12 yeast strain. All transformants containing the positive control Avr1b signal peptide (Avr1bSP) or the test Fg02685SP grew well on the CMD-W and YPRAA plates, indicating that the Fg02685 signal peptide had a secretion function (Figure 2a). However, the transformants with Fg02685^{ΔSP} (without the signal peptide) could not grow on the selective medium (Figure 2a). In addition, the enzyme activity of the secreted invertase from the transformants was detected in vivo. 2,3,5-triphenyl tetrazolium chloride was converted into the insoluble red-coloured 1,3,5-triphenyl formazan after adding yeast containing Avr1bSP or Fg02685SP, indicating that invertase was secreted from the yeast in the presence of the Fg02685 signal peptide (Figure 2a).

The entire length of Fg02685 and Fg02685^{ΔSP} tagged with GFP was used to detect the localization of Fg02685 after NaCl-induced

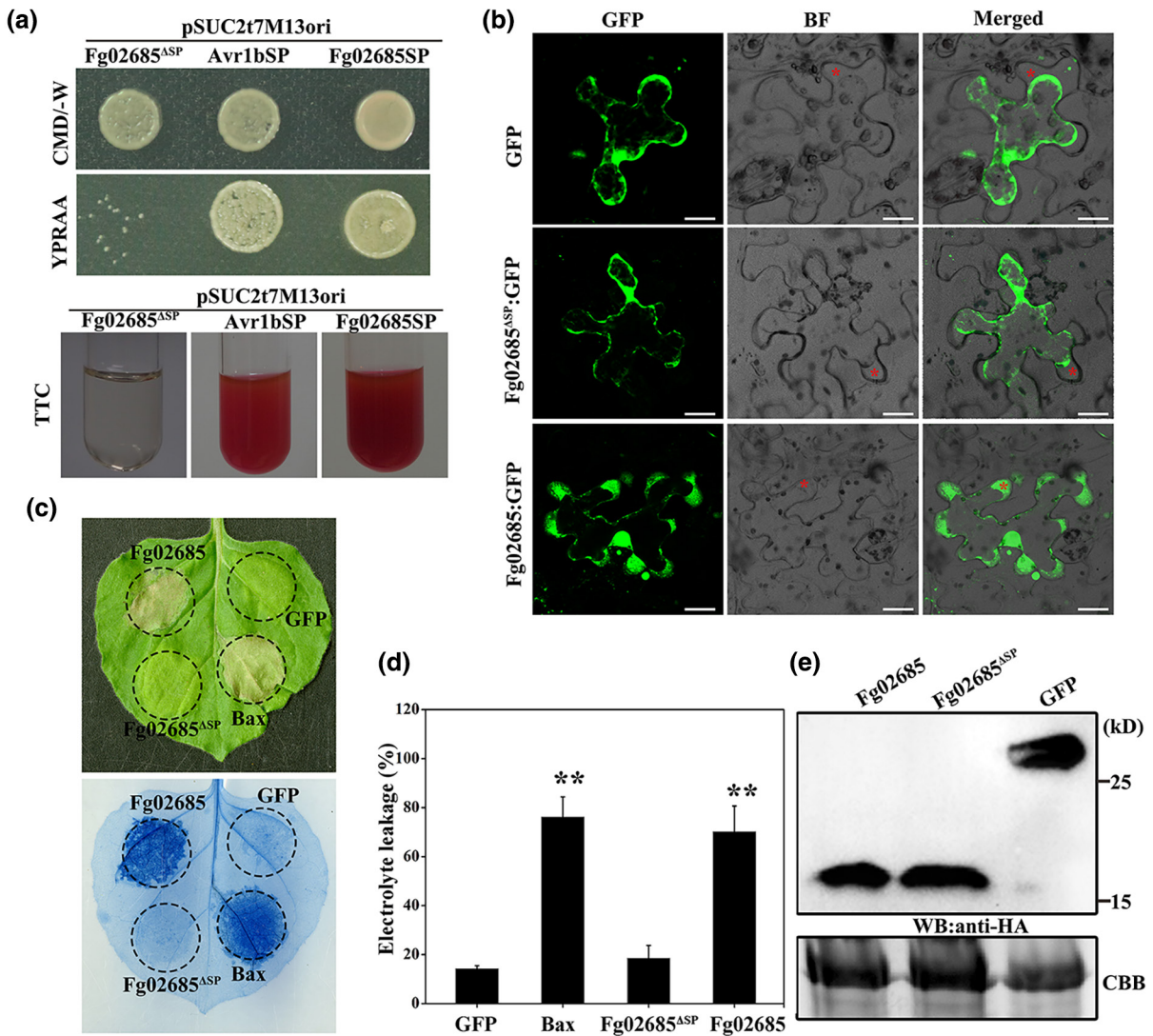


FIGURE 2 Functional evaluation of the Fg02685 signal peptide (Fg02685SP). (a) The functionality of Fg02685SP was tested using the yeast system containing the empty vector, Avr1bSP, or Fg02685SP. The transformants were cultured on CMD-W and YPRAA plates. The invertase enzymatic activity was detected by reducing 2,3,5-triphenyl tetrazolium chloride (TTC) to insoluble red-coloured 1,3,5-triphenyl formazan. (b) The full-length Fg02685 and Fg02685^{ASP} tagged with green fluorescent protein (GFP) and GFP alone were transiently expressed in *Nicotiana benthamiana*. Plant epidermis cells were treated with 70 mM NaCl for plasmolysis and analysed by confocal microscopy at 48 h after *Agrobacterium* infiltration. The asterisk indicates the apoplast region (bar = 20 μm). (c) Cell death detection on tobacco leaves after transient expression of Fg02685, Fg02685^{ASP}, GFP, and Bax. Representative images were taken at 5 days postinoculation (dpi). (d) Detection of electrolyte leakage in *N. benthamiana* leaves transiently expressing Fg02685, Fg02685^{ASP}, GFP, and Bax at 3 dpi. Asterisks indicate significant differences based on an unpaired two-tailed Student's *t* test ($p < 0.01$). (e) Fg02685:HA and GFP:HA proteins were detected by western blot (WB) with an anti-HA antibody. Coomassie brilliant blue (CBB) staining indicates equal loading.

plasmolysis to further confirm the function of the Fg02685 signal peptide in plants. Figure 2b shows that the GFP signals of Fg02685:GFP were observed in the *N. benthamiana* apoplast, while GFP was observed in both the cytoplasm and the nucleus instead of the apoplast region of cells expressing GFP and Fg02685^{ASP}:GFP (Figure 2b).

Fg02685^{ASP} was transiently expressed in *N. benthamiana* to test whether Fg02685 induced cell death in the plant apoplast. The results showed that the entire length of Fg02685 triggered cell death, whereas Fg02685^{ASP} could not induce cell death (Figure 2c). Loss of the signal peptide abolished the cell death-inducing function of Fg02685, as determined by quantifying ion leakage (Figure 2d). An

anti-HA antibody was used to confirm the Fg02685 and Fg02685^{ASP} expression levels in vivo (Figure 2e). These results suggested that the Fg02685 signal peptide is necessary for cell death-inducing activity.

2.3 | NbBAK1 and NbSOBIR1 are not required for Fg02685-induced cell death in *N. benthamiana*

Several cell death-inducing secreted proteins of fungi act as PAMPs and are recognized by pattern recognition receptors in the apoplast region and activate host defence responses (Heese et al., 2007;

Liebrand et al., 2013, 2014). Here, we tested whether the Fg02685-induced cell death in the apoplast region of the plant was mediated by the crucial central regulatory components BAK1, SOBIR1, and NDR1. Using tobacco rattle virus (TRV)-induced gene silencing (VIGS), the BAK1, SOBIR1, and NDR1 genes were first silenced. At 3 weeks after VIGS-mediated gene silencing, the silenced leaves were agroinfiltrated with Fg02685-, Bax-, or GFP-expressing constructs. Like the positive control Bax, Fg02685 did not lose its ability to induce cell death in the plants with BAK1, SOBIR1, or NDR1 silenced (Figures 3a and S3). A change in electrolyte leakage was observed around the region of Fg02685 and Bax infiltration when BAK1, SOBIR1, or NDR1 were silenced (Figure 3b). Compared to the control plants (pTRV2:GFP), the expression level of the receptor genes decreased by 65%–70% in plants expressing pTRV2:SOBIR1 and pTRV2:BAK1 (Figure 3d). Western blot analysis with anti-GFP confirmed the expression of GFP and Fg02685:GFP proteins in leaves inoculated with pTRV2:GFP, pTRV2:SOBIR1, and pTRV2:BAK1 (Figure 3c). Due to the similarity with the homologue VmE02, we also examined whether the Fg02685-induced cell death was mediated by the receptor REO2 (Nie et al., 2021). The results showed that Fg02685 also induced cell death in REO2-silenced plants (Figure S4). Taken together, these results indicated that Fg02685 could activate plant cell death independently of NbBAK1, NbSOBIR1, REO2, and NbNDR1.

2.4 | Fg02685 triggers plant immunity responses in *N. benthamiana*

Callose deposition was assessed after inducing transient expression Fg02685:GFP, Fg02685^{ΔSP}:GFP, and GFP alone in leaves to determine whether the cell death induced by Fg02685 was connected with plant defence priming. At 24 h post-agroinfiltration, aniline blue staining showed more callose deposition in the leaves expressing Fg02685:GFP than in leaves expressing GFP alone and Fg02685^{ΔSP}:GFP (Figure 4a). Moreover, Fg02685:GFP significantly activated callose foci, but Fg02685^{ΔSP}:GFP did not (Figure 4b). Fg02685:His protein was purified and tested for its ability to induce ROS accumulation in *N. benthamiana* leaves to further examine the plant defence response induced by Fg02685. The Fg02685:His protein had the ability to induce a ROS burst, like the flg22 peptide (Figure 4c). Furthermore, the expression levels of defence-related genes *NbPR1* and *NbPR2* were 16- and 20-fold higher, respectively, in leaves expressing Fg02685:GFP than in the control plants expressing GFP alone (Figure 4d). However, in the leaves expressing Fg02685^{ΔSP}:GFP, the transcript levels of these genes showed no difference compared with the control (Figure 4d). A hypersensitive response-specific gene (*NbHIN1*) and other PTI-related marker genes, including *NbWRKY7*, were then examined

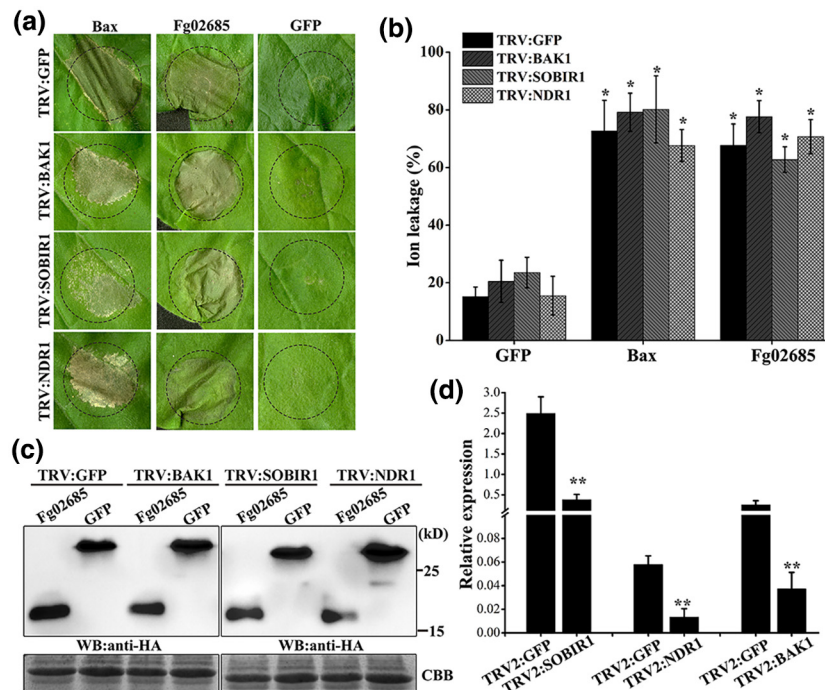


FIGURE 3 *NbBAK1* and *NbSOBIR1* are not required for Fg02685-induced cell death in *Nicotiana benthamiana*. (a) Cell death phenotype in BAK1-, SOBIR1-, or NDR1-silenced plants induced by Fg02685. The receptor genes were silenced by inoculating TRV2:GFP, TRV2:BAK1, TRV2:SOBIR1, or TRV2:NDR1. GFP or recombinant protein was transiently expressed in tobacco at 3 weeks after viral inoculation, and representative images were taken at 5 days postinoculation. (b) Electrolyte leakage was detected in leaves of the same set of plants as in Figure 4a. The mean and standard deviation were calculated with data from three independent replicates. Asterisks indicate significant differences based on the unpaired two-tailed Student's *t* test ($*p < 0.05$). (c) Fg02685:HA and GFP:HA proteins from *N. benthamiana* leaves, as shown in Figure 4a, were examined by western blot with an anti-HA antibody. Coomassie brilliant blue (CBB) staining indicates equal loading. (d) The expression levels of *NbBAK1*, *NbSOBIR1*, and *NDR1* were measured by reverse transcription-quantitative PCR. The mean and standard deviation were calculated with data from three independent replicates. Asterisks indicate significant differences based on the unpaired two-tailed Student's *t* test ($**p < 0.01$).

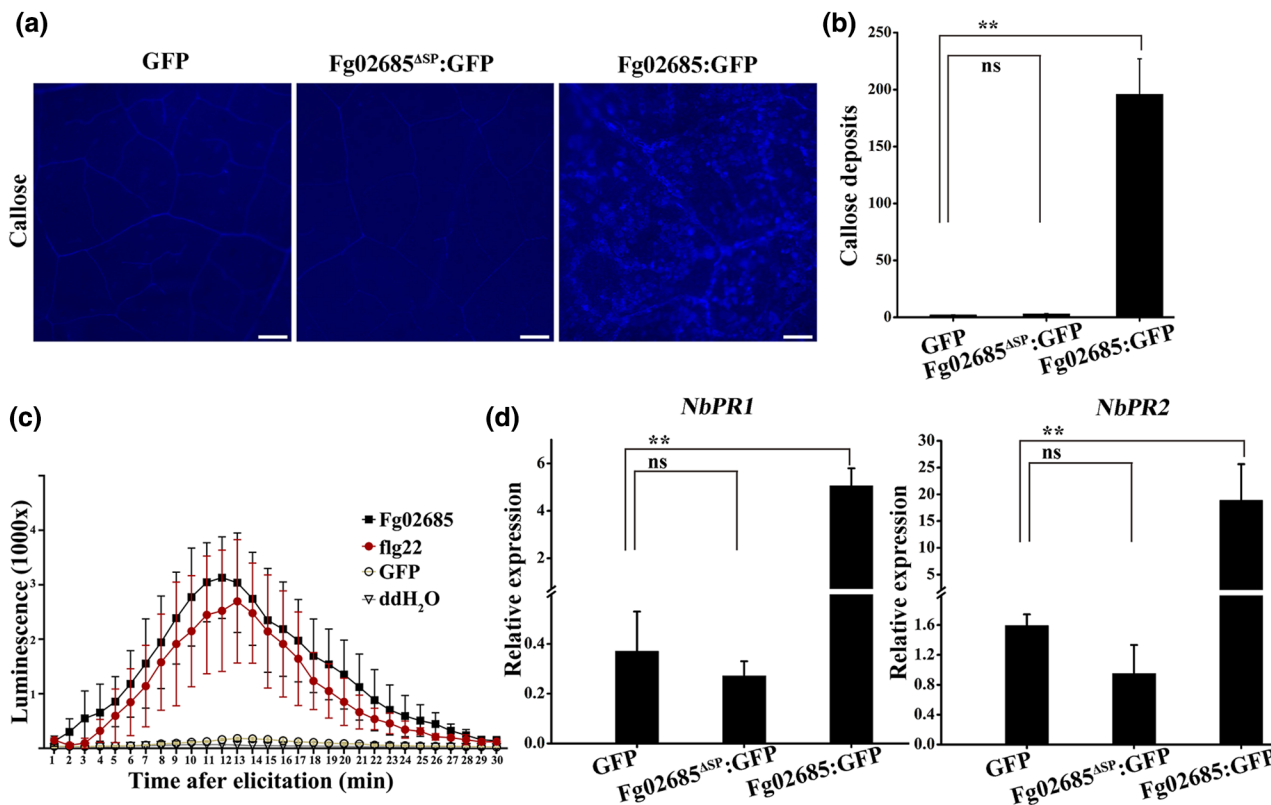


FIGURE 4 Activation of plant PAMP-triggered immunity (PTI) by Fg02685. (a) Detection of callose deposition induced by Fg02685 in *Nicotiana benthamiana*. Fg02685:GFP, Fg02685^{ΔSP}:GFP, and GFP alone were transiently expressed in *N. benthamiana* leaves. After 12 h, leaves were stained with 0.05% aniline blue. Representative pictures were collected using CellSens Entry software. Scale bar = 100 μ m. (b) Callose deposits per 1 mm² were assessed using ImageJ. The bar chart represents the average and standard deviation. Statistical significance relative to GFP control was assessed using an unpaired two-tailed Student's *t* test (***p* < 0.01; ns, not significant). (c) Total reactive oxygen species production in 60 min following treatment of *N. benthamiana* leaves with 1 μ M Fg02685 recombinant protein, GFP, or flg22. Error bars indicate standard deviation (*n* = 6). (d) Transcript levels of the PTI marker genes *NbPR1* and *NbPR2* were determined in *N. benthamiana* leaves as in Figure 5a. The mean and standard deviation were calculated from three biological replicates. Asterisks indicate significant differences based on the unpaired two-tailed Student's *t* test (***p* < 0.01; ns, not significant).

in leaves expressing Fg02685 via *Agrobacterium* (Qi et al., 2016). Analysis of the expression levels indicated that *NbHIN1*, *NbPti5*, and *NbWRKY7* were activated about seven-, two-, and threefold in the leaves expressing Fg02685:GFP compared to control plants expressing GFP or Fg02685^{ΔSP}:GFP, respectively (Figure S5). These results indicate that Fg02685 can activate plant defence responses.

2.5 | The α -helical motif at the N-terminus of Fg02685 is an elicitor-active epitope

A phylogenetic tree of 20 fungi was constructed to explore the distribution and conservation of Fg02685 homologues in fungi (Figure 5a). The results indicated that 67 sequences from biotrophic, necrotrophic, and hemibiotrophic pathogens showed high similarity in protein sequences (Figures 5a and S6a). About 80% of the protein sequences were found in pathogens of Poaceae species. About half of the sequences were from *Puccinia* species; compared with other pathogens, the number of homologues expanded broadly and their amino acid sequences were extended at the C-terminus (Figure S6b). In *F. graminearum*, Fg02685 is a single protein and its

sequence exhibits high similarity with oomycetes (Figure 5a). Given this conservation, the ability of some homologues to induce cell death was selectively tested. The homologous proteins from *Fusarium* (RBQ95317, XP_023431000, and QPC77170) and from *Phytophthora* (XP_009515305 and XP_008904024) triggered cell death (Figure S7). However, the protein from *Puccinia sorghi* (KNZ58081) and the protein from *Puccinia striiformis* (KNE89953) failed to induce cell death (Figure S7). *N. benthamiana* was found to recognize the homologous proteins of Fg02685.

The secondary structure motifs of Fg02685 showed two α -helical motifs and a five-stranded β -barrel fold without a conserved domain (Figure 5b). To test whether Fg02685-induced cell death was linked with these structures, the amino acids in the α -helix and β -sheet were changed to alanine (A) to break the corresponding secondary structure (Figure 5b). Fg02685^{Δ6A}, Fg02685^{Δ7A}, and Fg02685^{Δ8A} were expressed in *N. benthamiana* leaves to characterize their function. Compared with Fg02685, Fg02685^{Δ6A} failed to induce cell death (Figure 5c). In addition, a significant change in electrolyte leakage was observed when Fg02685^{Δ7A} and Fg02685^{Δ8A} were expressed (Figure S8a). Fg02685 was divided into the N-terminus Fg02685^{Δ60-147} (α -helix) and the C-terminus Fg02685^{Δ19-59} (Figure 5b). Fg02685^{Δ60-147} could

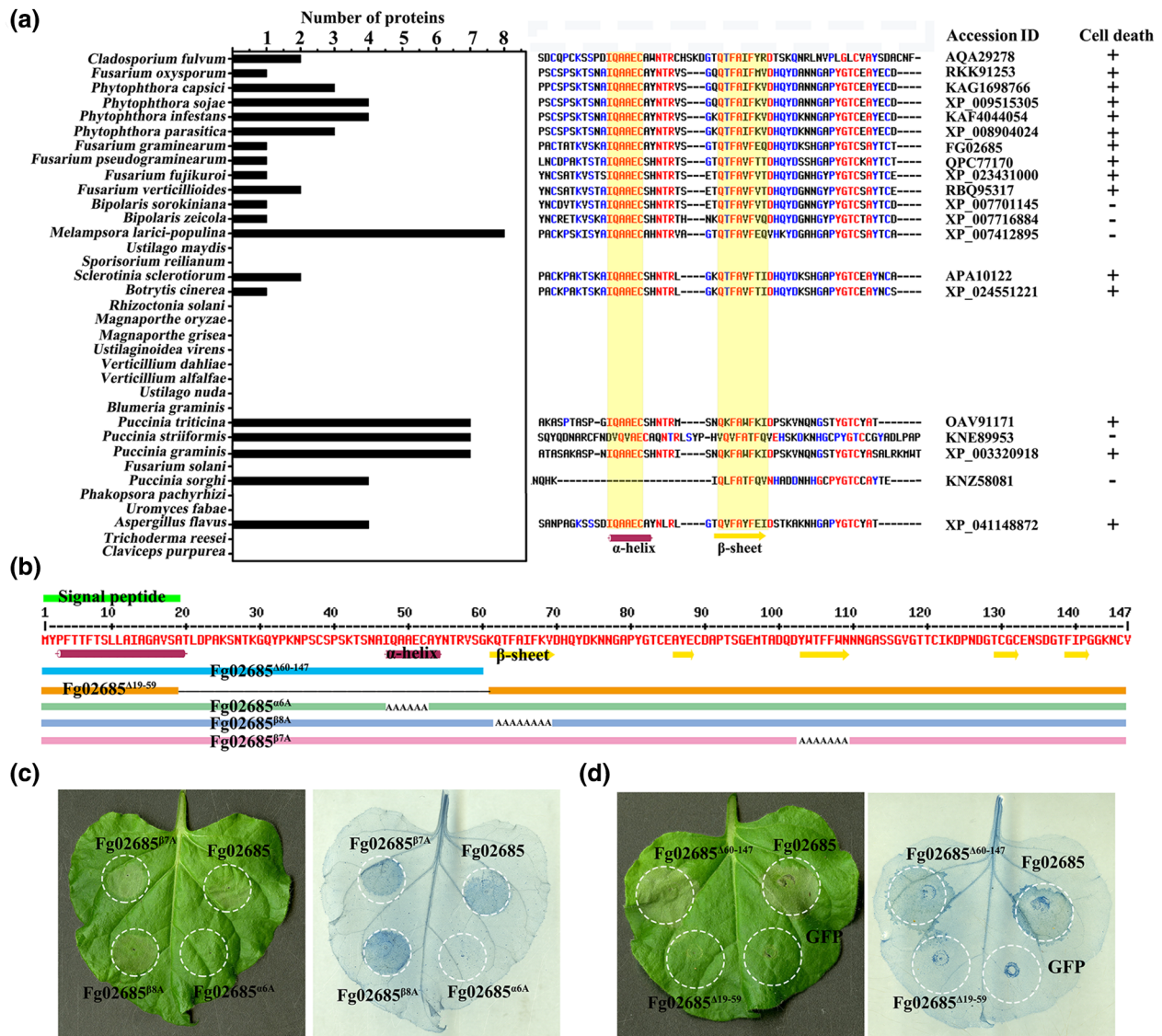


FIGURE 5 The conserved N-terminus of Fg02685 is sufficient to induce cell death in *Nicotiana benthamiana*. (a) Distribution of Fg02685 homologues in various pathogens. The number of homologous proteins was labelled in selected species (left), and the conserved homologues of Fg02685 from oomycetes- and *Fusarium*-induced cell death in *N. benthamiana* (right). (+) cell death, (-) no clear cell death. (b) A schematic diagram of Fg02685 fragments tested for cell death-inducing activity. The FgNP32 peptide was artificially synthesized. (c) The conserved IQAAEC motif (α -helix) was required for the induction of cell death. The leaves were treated with trypan blue solution and cell death symptoms were visualized. Representative photographs were observed at 3 days postinoculation (dpi). (d) The conserved N-terminus of Fg02685 also elicited plant cell death. Fg02685 was artificially divided into the N-terminus Fg02685 ^{Δ 60-147} and the C-terminus Fg02685 ^{Δ 19-59}. The cell death phenotype was observed at 3 dpi.

induce cell death while Fg02685 ^{Δ 19-59} could not (Figure 5d), indicating that the α -helix structure at the N-terminus of Fg02685 is sufficient to induce cell death. Consistent with these results, a significant increase in the electrolyte leakage was observed around the region of Fg02685 ^{Δ 60-147} expression (Figure S8b).

2.6 | Fg02685 contributes to the virulence of *F. graminearum*

The transcript levels from conidia, vegetative hyphae, and several important early infection stages of the wheat head were evaluated

to investigate the potential role of Fg02685 during the wheat-*F. graminearum* interaction. Figure S9 shows that Fg02685 was induced by 8- to 16-fold compared with the control at 48 h postinoculation (hpi) and then decreased to a lower level of two- to threefold change compared with the control at 72-120 hpi (Figure S9). These results suggested that Fg02685 is highly induced during *F. graminearum* infection.

Fg02685 Δ SP was transiently expressed in *N. benthamiana* to test whether Fg02685 induced cell death in the plant apoplast. Fg02685 knockout mutants, in which the Fg02685 gene was replaced with the hygromycin resistance gene, and its complementation strain were generated to assess the function of Fg02685 in *F. graminearum* virulence

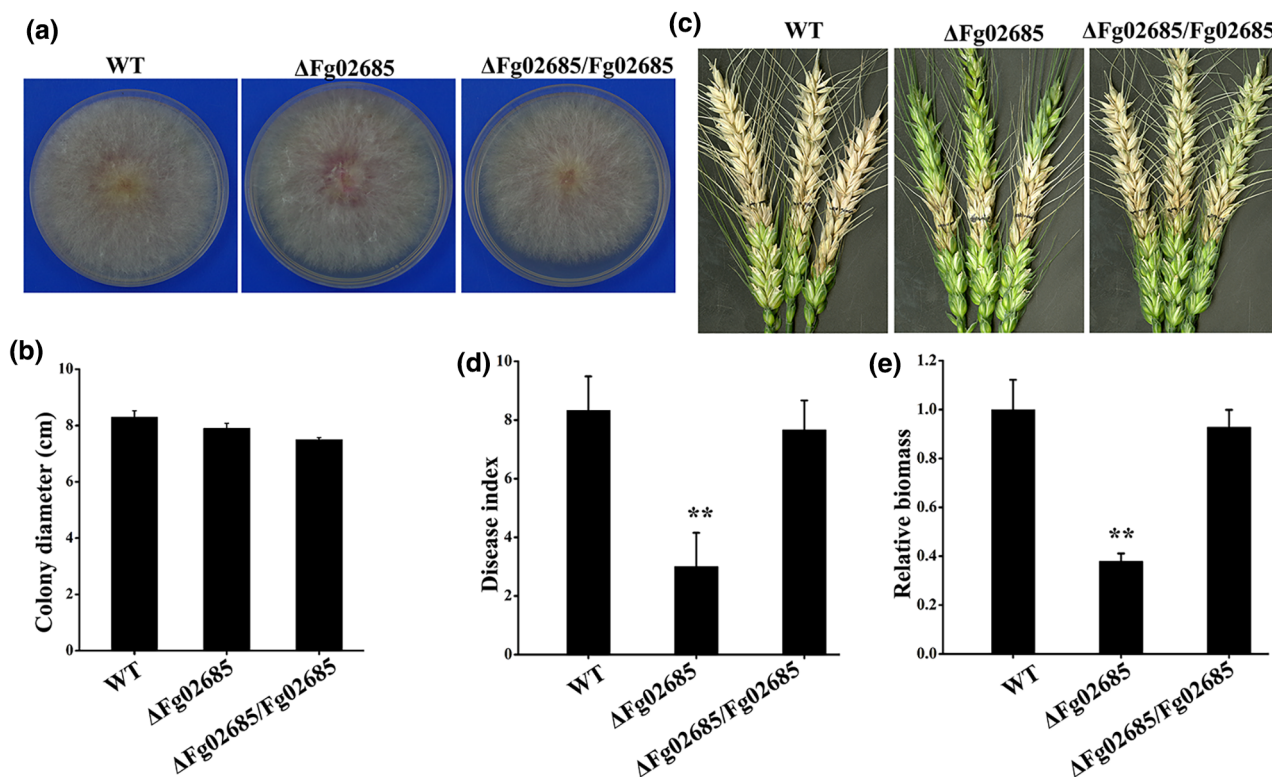


FIGURE 6 Fg02685 is essential for the virulence of *Fusarium graminearum*. (a) The mycelial phenotypes of the wild type (WT), Δ Fg02685 mutant, and Δ Fg02685/Fg02685 complementation transformants cultured on potato dextrose agar at 25°C for 4 days. (b) Colony diameter of WT, Δ Fg02685 mutant, and Δ Fg02685/Fg02685 transformants. The mean and standard deviation were calculated from three biological replicates. (c) Wheat heads and rhizomes were inoculated with WT, Δ Fg02685, and Δ Fg02685/Fg02685. Representative images were taken at 14 days postinoculation (dpi). (d) The disease index of WT, Δ Fg02685 mutant, and Δ Fg02685/Fg02685 transformants. The mean and standard deviation were calculated with data from three independent replicates with at least six wheat heads examined in each experiment. Asterisks indicate a significant difference based on the unpaired two-tailed Student's *t* test (** $p < 0.01$). (e) Fungal biomass in infected wheat heads at 5 dpi was determined by real-time PCR. The mean and standard deviation were calculated with data from three independent replicates. The asterisks indicate significant difference in comparison with the control (** $p < 0.01$).

(Figure S10). No difference was observed in the hyphal growth rate and colony morphology of the Fg02685 knockout strain and its complementation strain compared with the wild type (WT) (Figure 6a,b). However, the disease symptoms were less severe after inoculation with the Fg02685 knockout strain (Figure 6c). The number of diseased spikelets was lower in plants treated with the Fg02685 knockout strain than in plants inoculated with the WT strain (Figure 6d). To further assess the development of *F. graminearum*, its biomass was determined and was found to be markedly lower than that of the WT strain (Figure 6e). However, the Fg02685 complementation strain exhibited restored biomass, comparable to WT levels (Figure 6c–e). Therefore, these results indicate that Fg02685 contributes to the virulence of *F. graminearum*.

2.7 | FgNP32 induced the basal immune response in plants

Most homologous proteins that possessed the ability to induce cell death had an α -helix structure at the N-terminus (Figure 5a). Therefore, FgNP32 was synthesized, and its ability to trigger cell death in plants was tested to identify the minimal immunogenic epitope of Fg02685.

N. benthamiana leaves were pretreated with 1 μ M FgNP32 or flg22 (as a positive control) to test whether FgNP32 activated plant immunity. More abundant callose deposits were observed in leaves treated with FgNP32 than in control leaves (Figure 7a). Chemiluminescent detection of the oxidative burst showed that ROS accumulation was significantly increased in *N. benthamiana* leaves treated with FgNP32 (Figure 7b). Further evidence of the effects of FgNP32 on the induction of plant defence was obtained by examining MAPK phosphorylation and the expression of pathogenesis-related genes. Like in leaves treated with flg22, MAPK phosphorylation was also confirmed in leaves treated with the FgNP32 peptide (Figure 7c). In addition, after flg22 and FgNP32 infiltration in repeated experiments, the transcript levels of the pathogenesis-related genes *NbPR1*, *NbPR2*, and *NbWRKY* were 6-, 10-, and 10-fold higher, respectively (Figure 7d), indicating that PTI was triggered in the leaves.

2.8 | FgNP32 enhances disease resistance in plants

The induction of disease resistance in *N. benthamiana* against *Phytophthora parasitica* var. *nicotianae* was first examined to test

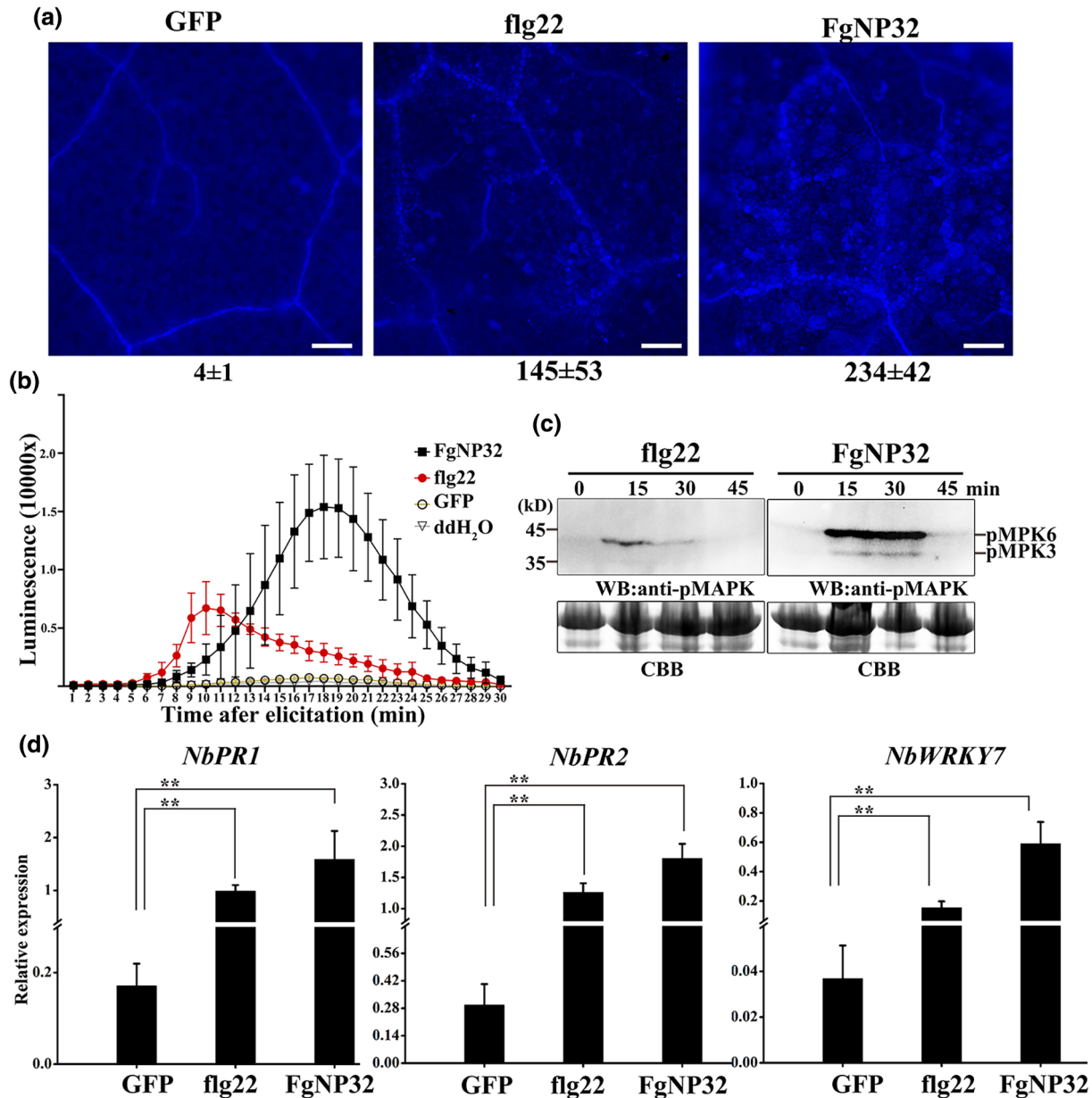


FIGURE 7 The plant PAMP-triggered immunity (PTI) induced by FgNP32. (a) Detection of callose deposition in *Nicotiana benthamiana* after 12h of treatment with 1 μ M FgNP32 or flg22. Leaves were stained with 0.05% aniline blue. Representative pictures were collected using CellSens Entry software. Scale bar = 100 μ m. The number of callose deposits per mm² was determined using ImageJ. The mean and standard deviation were calculated from three biological replicates. (b) Total reactive oxygen species accumulation in the 60 min following treatment of *N. benthamiana* leaves with 1 μ M FgNP32, GFP, or flg22. Error bars indicate standard deviation ($n = 6$). (c) FgNP32- and flg22-induced MAPK activation in *N. benthamiana*. The leaves were infiltrated with 1 μ M FgNP32 or flg22, and total proteins were extracted for immunoblotting with an anti-pERK1/2 antibody. Protein loading is indicated by Coomassie brilliant blue (CBB) staining. (d) Transcript levels of PTI marker genes *NbPR1*, *NbPR2*, and *NbWRKY7* were measured in *N. benthamiana* as in Figure 7a. The mean and standard deviation were calculated from three biological replicates. Asterisks indicate significant differences based on the unpaired two-tailed Student's *t* test (** $p < 0.01$).

whether FgNP32 enhanced disease resistance in plants. Figure 8a shows that the disease lesions were significantly reduced in the *N. benthamiana* leaves treated with 1 μ M FgNP32 compared with the controls. In repeated experiments on soybean hypocotyl inoculation with *P. sojae*, pretreatment with FgNP32 significantly enhanced soybean resistance to *P. sojae*. Quantitative real-time PCR (qPCR) analysis confirmed that the disease lesions and *Phytophthora* biomass decreased compared with the control treated with GFP (Figure 8b).

Then, the disease resistance to bacteria in *N. benthamiana* leaves was also tested. As shown in Figure S11, the disease lesions were significantly reduced and *Pseudomonas syringae* pv. *tomato* DC3000 growth was twofold lower in the *N. benthamiana* leaves treated with 1 μ M FgNP32 compared with that of the control. These results indicated that FgNP32 activated plant immunity in *N. benthamiana* and soybean.

The same experiments were performed on wheat coleoptiles to conduct a more detailed analysis of disease resistance in host

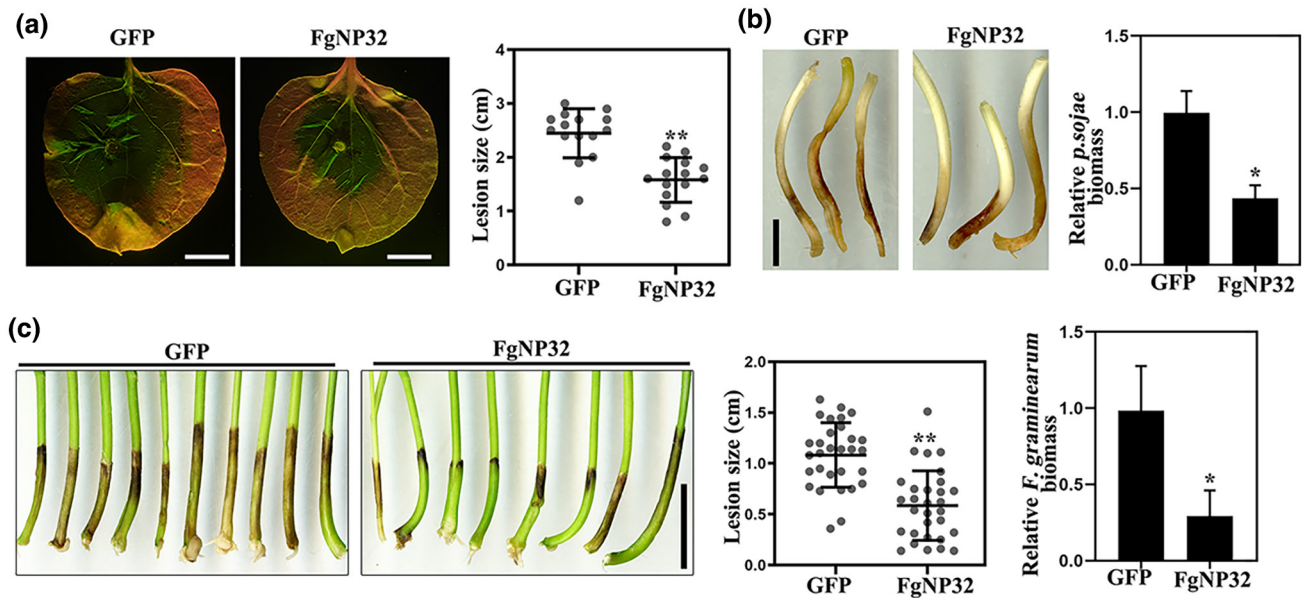


FIGURE 8 FgNP32 induces disease resistance in plants. *Nicotiana benthamiana* leaves, wheat coleoptiles, and soybean hypocotyl were treated with 1 μ M FgNP32 peptide 12h prior to inoculation with pathogens. (a) The phenotypes of *N. benthamiana* leaves at 48h postinoculation (hpi) with *Phytophthora parasitica* var. *nicotianae*. Lesions of the same leaves were analysed at 48hpi. Bar = 1 cm. Lesion diameters were assessed from three independent experiments ($n = 15$). (b) The disease symptoms of soybean hypocotyls at 2 days postinoculation (dpi) with *Phytophthora sojae*. Bar = 1 cm. Fungal biomass was measured by quantitative PCR (qPCR). The mean and standard deviation were calculated from three independent experiments. (c) Representative pictures of disease lesions of wheat coleoptiles were captured at 7 dpi with *Fusarium graminearum*. Mean lengths were calculated from three biological replicates ($n = 30$). Bar = 1 cm. Fungal biomass was quantified by qPCR. Asterisks indicate significant differences based on an unpaired two-tailed Student's *t* test ($*p < 0.05$; $**p < 0.01$).

plants. When coleoptiles of 3- to 4-day-old wheat seedlings were treated with FgNP32 before inoculation with *F. graminearum*, dark brown lesions were shorter at 7dpi than the lesions in coleoptiles treated with GFP alone (Figure 8c). FgNP32 significantly decreased the pathogen biomass after coleoptile infection with *F. graminearum*. Taken together, these results indicated that FgNP32 enhanced resistance in wheat coleoptiles to *F. graminearum* infection.

3 | DISCUSSION

Compared with other model fungal pathosystems, the *F. graminearum*-wheat interaction process has particular traits. The infected hyphae of *F. graminearum* can encircle the plant cell extracellularly without visible disease symptoms in the initial stages (Brown et al., 2017). At this stage, the pathogens optimize the spatiotemporal deployment of various effector proteins to modulate the host innate immunity for its colonization, which is similar to an apoplastic biotroph. Spatiotemporal transcriptome analysis showed about 18 effectors with elevated expression, although many effectors have not been tested (Brown et al., 2017). Interestingly, Fg02685 might not function in this period because its transcription level was not significantly upregulated at the early infection stage. In contrast, its expression rapidly increased 8- to 16-fold, in line with the transcriptome analysis results, at later infection stages when *Fusarium* effectors may be involved in the stimulation of host cell death for nutrient uptake and cell-to-cell hyphal invasion (Jia et al., 2019).

In this study, Fg02685 was identified as a small secreted protein without a conserved domain to be delivered into the extracellular region to induce cell death in various plants. Although knockout of Fg02685 weakened the virulence of *F. graminearum* during infection, transiently expressed Fg02685 could stimulate the plant basal immune response. This seems contradictory, but Fg02685 with lower transcription levels evaded recognition by plant receptors at the early infection stage and assisted in the induction of cell death when the infected hyphae penetrated plant cells for the proliferation of fungal biomass. This study also indicated that *Fusarium* finely coordinated temporal expression of virulence factors and optimized allocation of gene resources.

A large body of emerging evidence indicates effectors secreted by the pathogens are a set of crucial pathogenicity factors to regulate plant immunity and promote their colonization (He et al., 2018; Ishikawa et al., 2014). About 292 secreted effectors have been identified in the *F. graminearum* genome (Brown et al., 2012; Sperschneider et al., 2016). Currently, knowledge of the function of its secreted effectors is markedly poor except for the secreted protein OSP24 and lipase FGL1 (Blümke et al., 2014; Jiang et al., 2020). In this study, a small secreted protein, Fg02685, was identified to induce cell death in various plants. Recently, Fg12 was identified as an RNase secreted by *F. graminearum*, which significantly induced cell death in plants depending on its RNase enzymatic activity (Yang et al., 2021). Unlike Fg12, Fg02685 mainly accumulated in the plant apoplast. Fg02685^{ΔSP} failed to induce cell death in plants. In addition, like other PAMPs, transiently expressed Fg02685 stimulated a

series of plant immune responses by increasing ROS levels, MAPK signalling, and the expression of defence-related genes, indicating that Fg02685 acts as a microbial PAMP in filamentous pathogens. Among other PAMPs, SGP1 from *Ustilagoideae virens* induces cell death and provokes an immune response in rice leaves as a proteinaceous PAMP in a BAK1-dependent manner (Song et al., 2021). VmE02 from *Valsa mali* is recognized by receptor-like protein RE02-induced plant cell death (Nie et al., 2019, 2021). However, the plant defence response induced by Fg02685 is independent of the conserved receptors BAK1, SOBIR1, and RE02, indicating that other plant basal immune pathways induced by Fg02685 may work in parallel with the BAK1-, SOBIR1-, and NDR1-mediated system.

Fg02685 homologous proteins are widely distributed in filamentous pathogens and oomycetes, especially in *Puccinia* and *Phytophthora*. The proportion of homologous sequences in rust fungi is the largest, accounting for about 50%, including wheat rust and poplar rust. However, compared to other fungi, only one copy of Fg02685 was found in *F. graminearum*. Not all homologues induced cell death symptoms in the leaves expressing these proteins, for example from biotrophic fungi, *Puccinia*. Another phenomenon is that *Fusarium* contained only two homologous proteins, whereas *Puccinia* had eight. Cell death confers an evolutionary disadvantage to biotrophic fungi that derive nutrients from living plant cells. Thus, one hypothesis is that biotrophic fungi have evolved an expansion of the homologues with low similarity and lost their immunogenic epitopes in order to play different roles, due to selection pressures of plant immunity. Furthermore, the amino acid sequences of the homologues from biotrophic fungi were extended at the C-terminus. Second, the corresponding receptor in *N. benthamiana* might not be present to recognize the immunogenic epitope of homologues. Third, due to evolutionary driving forces, the homologous proteins from *Phytophthora* or *Fusarium* that could infect several plants, such as *N. benthamiana*, may also harbour the conserved C-terminus and have the ability to induce cell death. The spatiotemporal deployment of these factors circumvents plant immune monitoring for fungal development during the co-evolution of pathogen and host although many biotrophic, necrotrophic, and hemibiotrophic pathogens have secreted proteins that induce plant cell death.

Fusarium head blight (FHB) causes significant wheat yield losses worldwide. FHB resistance genes have been identified and cloned, for example, *Fhb1*, *ICS*, and *NAC* (Hao et al., 2018; Perochon et al., 2019). *Fhb1*, a quantitative trait locus, provides a stable influence on FHB resistance in wheat, and mutation of a putative histidine-rich calcium-binding protein gene confers head blight resistance (Li et al., 2019; Su et al., 2019). However, the development of FHB-resistant cultivars has not been very successful because of the complicated plant resistance mechanisms and limitations of germplasm. Furthermore, excessive traditional fungicide use leads to environmental pollution and increased pathogenic resistance. The application of green and non-polluting agents seems promising in the foreseeable future. Generally, some microbe elicitors are regarded as environmentally friendly biological reagents enhancing plant disease resistance. The foliar spray of chitosan on barley induces localized resistance in the leaf against

powdery mildew and activates systemic tobacco resistance to necrosis virus (Faoro et al., 2008; Iriti et al., 2006). Guanine from a crude extract of the endophyte was recently identified as a plant immune inducer to enhance plant resistance to rice sheath blight, depending on the ethylene pathway (Wang et al., 2022). In our study, Fg02685 was identified as an elicitor from *Fusarium* and induced plant immunity. Treatment with exogenous FgNP32, a 32-amino-acid peptide from the N-terminus of Fg02685, contributed to plant resistance against *Phytophthora*, *P. syringae*, and *Fusarium* in *N. benthamiana* and wheat, indicating that FgNP32 could act as a plant immune inducer to achieve durable disease control. This study provided evidence that the exploitation of induced plant resistance by the application of a novel bioactive immune inducer could be an attractive alternative for controlling crop diseases.

4 | EXPERIMENTAL PROCEDURES

4.1 | Biological materials and culture conditions

Wheat (*Triticum aestivum*) cultivar SM482 was cultured at 20–25°C, and *N. benthamiana* was grown in a phytotron at 22°C under a 16 h light/8 h dark cycle. *F. graminearum* was grown on potato dextrose agar (PDA) at 25°C. *Agrobacterium tumefaciens* GV3101 and AGL1 as well as *E. coli* DH5a were cultured in Luria–Bertani medium at 28°C and 37°C, respectively. The sequences of Fg02685 homologues were artificially synthesized by GENERAL Biology Company (Anhui, China). The FgNP32 peptide was synthesized by GenScript Biotech Company (Nanjing, China).

4.2 | Sequence analysis and transcript levels

For sequence analysis, the signal peptide of Fg02685 was predicted using SignalP v. 4.0. ApoplastP software was used to predict the sublocalization. The secondary structure was tested using Jpred 4. The sequence alignment was established by the MULTALIN website (<http://multalin.toulouse.inra.fr/multalin/multalin.html>). For the expression analysis of Fg02685, wheat heads infected with *F. graminearum* at 12, 24, 36, 72, 96, and 120 hpi, conidia of *F. graminearum* from 5-day-old carboxymethyl cellulose cultures, and fungal hyphae from 4-day-old PDA cultures were harvested for RNA extraction using the MiniBEST Plant RNA Extraction Kit (TaKaRa Bio Inc.) following the manufacturer's instructions. Genomic DNA was extracted using the CTAB method for sequence amplification. qPCR was performed using a Bio-Rad CFX Manager (v. 3.1) under the corresponding conditions. *TaGAPDH* for wheat, *FgActin* for *F. graminearum*, and *NbActin* for *N. benthamiana* were used as the internal reference genes for reverse tra-qPCR.

4.3 | Protein expression in *N. benthamiana*

For the cell death assay, *A. tumefaciens* GV3101 carrying PVX:Fg02685:HA, PVX:eGFP:HA, or PVX:Bax was washed three

times with 10mM MgCl₂ and diluted to an optical density at 600 nm (OD₆₀₀) of 0.4. The corresponding strains were infiltrated into plant leaves using a 1-ml syringe. For localization in *N. benthamiana*, Fg02685:GFP and Fg02685^{ASP}:GFP were transformed into *A. tumefaciens*, and the bacterial suspension with OD₆₀₀ = 0.6 was injected into 4-week-old *N. benthamiana* leaves and kept in the glasshouse at 22°C. At 48 hpi, the epidermis of leaves was treated with 70mM NaCl for 10–20 min and then observed by confocal microscopy.

4.4 | Transient expression of proteins in yeast

The signal peptide sequence was cloned into the pSUC2 vector, which carries the sucrose invertase gene *SUC2* without the initiation ATG codon and the signal peptide sequence and was transformed into yeast YTK12 (Jacobs et al., 1997). The transformant strains were then screened on CMD-W plates (0.67% yeast nitrogen base, 2% sucrose, 0.1% glucose, 2% agar, 0.075% tryptophan dropout supplement) and selective YPRAA plates (1% yeast extract, 2% peptone, 2% raffinose, 2 µg/ml antimycin A, 2% agar). YTK12 strains with empty pSUC vector or pSUC2-Avr1bSP were used as negative and positive controls, respectively. The enzymatic activity was tested by reducing 2,3,5-triphenyl tetrazolium chloride to red 1,3,5-triphenyl formazan.

4.5 | Plant cell death and ROS detection

For detection of cell death by trypan blue staining (Qi et al., 2016), the corresponding leaves were treated with trypan blue solution (0.02% trypan blue in phenol-glycerol-lactic acid-water-ethanol at 1:1:1:1:8, vol/vol/vol/vol/vol) at 95°C for 5 min. The leaves were decoloured using chloral hydrate solution. For electrolyte leakage measurements, four leaf discs from infiltrated areas with a diameter of 1 cm were floated in 10 ml distilled water for 10 h, and the conductivity was tested by a conductivity meter (DDS-307; LEICI) (value A). The leaf discs were boiled for 20 min. When the solution cooled to room temperature, the conductivity was measured again (value B). Ion leakage was calculated as A/B. To detect ROS, *N. benthamiana* leaves with a size of 1 cm² were collected into a 96-well plate and maintained overnight with 200 µl water to eliminate physical damage-induced ROS. The leaves were treated with 200 µl of solution containing 37.5 µg/ml luminol, 25 µg/ml horseradish peroxidase, and 1 µM of Fg02685, flg22, or FgNP32. Luminescence was tested using a multiscan spectrum (Varioskan LUX) at 562 nm for 60 min. For each data point six replicates were measured, and the experiments were repeated three times.

4.6 | MAPK assay

Total protein was extracted from *N. benthamiana* leaves treated with 1 µM FgNP32 or flg22 using a plant phosphorylated protein

extraction kit (HR0011; Baiao Laibo) as directed by the manufacturer. The phosphorylated protein in the MAPK pathway was detected by western blot with an anti-pERK1/2 antibody (AF1891; Beyotime Biotechnology). Protein loading was checked by staining with Coomassie brilliant blue R-250 (Beyotime Biotechnology).

4.7 | VIGS assay in *N. benthamiana*

For silencing *NbBAK1* and *NbSOBIR1*, the specific fragments were cloned into pTRV2 and transformed into *A. tumefaciens* GV3101. The bacteria with pTRV1 and pTRV2:GFP or pTRV2:PDS, pTRV2:BAK1, and pTRV2:SOBIR1 were infiltrated into *N. benthamiana* leaves with OD₆₀₀ = 1.0. pTRV2:GFP and pTRV2:PDS were used as control. At 2 weeks after infiltration, *N. benthamiana* leaves were agroinfiltrated with Fg02685, GFP, or *Bax* to detect cell death. RNA was extracted from three leaves for the assessment of silencing efficiency.

4.8 | Protein expression and purification in *E. coli*

The Fg02685 sequence was inserted into the pET-28a vector, which was transformed into *E. coli* BL21. The crude His-tagged Fg02685 proteins were purified by Ni-chelating affinity chromatography (17531802; General Electric Company). The concentration of Fg02685 was determined by the BCA protein concentration assay kit (Beyotime).

4.9 | Transformation of *F. graminearum* and pathogenicity assay

For transformation of *F. graminearum*, the upstream and downstream fragments of the Fg02685 DNA sequence were selected and inserted into the Prf-HU2 vector, respectively. *A. tumefaciens* carrying the gene replacement construct Prf-HU2:Fg02685 and *F. graminearum* were co-cultured as described previously for transformation (Maier et al., 2005). For complementation assays, the entire Fg02685 gene with its native promoter was cloned into the pFL2 vector and then transformed into ΔFg02685 mutants (Zhou et al., 2011). The ΔFg02685/Fg02685 transformant was confirmed by PCR and tested for phenotype complementation. The WT strains and mutants were grown on PDA at 25°C to measure the growth rate and determine colony morphology. All the primers used in this study are mentioned in Table S2. For pathogenicity assays of *F. graminearum* (Jonkers et al., 2012), conidia of *F. graminearum* were obtained from a 5-day-old CMC culture and resuspended as 10⁵ spores/ml in sterile distilled water. The fifth wheat spikelets were then inoculated with 10 µl of spore suspension and sealed with a plastic wrap for 48 h to keep the humidity high. The phenotype of wheat heads inoculated with *F. graminearum* was examined at 14 dpi to determine the disease index. For fungal biomass measurements, total genomic DNA was extracted from the infected wheat

heads sampled at 5 dpi for qPCR assays. *TaEF-1α* and *FgCHS5* genes were used to normalize the RNA level of wheat and *F. graminearum*, respectively. For *N. benthamiana* inoculated with *P. parasitica*, the detached leaves were treated with 1 μM FgNP32 12h before infiltration with 10 μl of spore suspension (500 spores of *P. parasitica*), and the humidity was maintained with a wet paper for 2 days in the dark at 25°C. For *P. sojae* inoculated on soybean, etiolated soybean seedlings were treated with 1 μM FgNP32 in the dark for 12h, and the hypocotyls were inoculated with *P. sojae* in the dark for 48h. Disease symptoms were photographed at 96 hpi. For *N. benthamiana* inoculated with *P. syringae*, the leaves were treated with 1 μM FgNP32 12h before infiltration with 10 μl (number of bacteria: 10⁴) of bacterial suspension. For wheat coleoptiles treated with *F. graminearum*, the seeds of SM482 were cultivated at 22°C under a 16h light/8h dark cycle as described previously (Jia et al., 2017). About 10 μl of spore suspension (10⁶/ml) was inoculated on wheat coleoptiles or florets. Phenotypes were photographed 7 days after treatment with *F. graminearum*.

AUTHOR CONTRIBUTIONS

S.H., M.J., and Q.X. designed the research. S.H., M.J., and Y.X. conducted the experiments. S.H. constructed vectors and cultured tobacco and wheat plants. J.M., Y.Z., G.C., P.Q., and Y.Z. provided technical support. Q.X., S.H., and Y.W. analysed data. Y.W. and Q.X. wrote and revised this manuscript.

ACKNOWLEDGEMENTS

We thank Prof. Weihua Tang and Dr. Wanqiu Wang from the Institute of Plant Physiology and Ecology, Chinese Academy of Sciences for technical support with wheat coleoptile inoculation. We also thank Dr. Shulin Cao from the Institute of Plant Protection, Jiangsu Academy of Agricultural Sciences for providing the pFL2 vector. This study was supported by the National Natural Science Foundation of China (32102229), the Applied Basic Research Programs of Science and Technology Department of Sichuan Province, China (2021YJ0298), and the Sichuan Science and Technology Program, China (2022ZDZX0014).

CONFLICT OF INTEREST

The authors declare no competing interests.

DATA AVAILABILITY STATEMENT

The data that supports the findings of this study are available in the supplementary material of this article.

ORCID

Qiang Xu  <https://orcid.org/0000-0002-8433-8687>

Youliang Zheng  <https://orcid.org/0000-0003-2042-6538>

REFERENCES

- Audenaert, K., Vanheule, A., Höfte, M. & Haesaert, G. (2014) Deoxynivalenol: a major player in the multifaceted response of *Fusarium* to its environment. *Toxins*, 6, 1–19.
- Bailey, B.A. (1995) Purification of a protein from culture filtrates of *Fusarium oxysporum* that induces ethylene and necrosis in leaves of *Erythroxylum coca*. *Phytopathology*, 85, 1250–1255.
- Blümke, A., Falter, C., Herrfurth, C., Sode, B., Bode, R., Schäfer, W. et al. (2014) Secreted fungal effector lipase releases free fatty acids to inhibit innate immunity-related callose formation during wheat head infection. *Plant Physiology*, 165, 346–358.
- Boenisch, M.J. & Schäfer, W. (2011) *Fusarium graminearum* forms myco-toxin producing infection structures on wheat. *BMC Plant Biology*, 11, 110.
- Brown, N.A., Antoniw, J. & Hammond-Kosack, K.E. (2012) The predicted secretome of the plant pathogenic fungus *Fusarium graminearum*: a refined comparative analysis. *PLoS One*, 7, e3371.
- Brown, N.A., Evans, J., Mead, A. & Hammond-Kosack, K.E. (2017) A spatial temporal analysis of the *Fusarium graminearum* transcriptome during symptomless and symptomatic wheat infection. *Molecular Plant Pathology*, 18, 1295–1312.
- Brunner, F., Rosahl, S., Lee, J., Rudd, J.J., Geiler, C., Kauppinen, S. et al. (2002) Pep-13, a plant defense-inducing pathogen-associated pattern from *Phytophthora* transglutaminases. *The EMBO Journal*, 21, 6681–6688.
- Chen, X.-R., Huang, S.-X., Zhang, Y., Sheng, G.-L., Li, Y.-P. & Zhu, F. (2018) Identification and functional analysis of the NLP-encoding genes from the phytopathogenic oomycete *Phytophthora capsici*. *Molecular Genetics and Genomics*, 293, 931–943.
- Chinchilla, D., Zipfel, C., Robatzek, S., Kemmerling, B., Nürnberger, T., Jones, J.D.G. et al. (2007) A flagellin-induced complex of the receptor FLS2 and BAK1 initiates plant defence. *Nature*, 448, 497–500.
- Deising, H.B., Rauscher, M., Haug, M. & Heiler, S. (1995) Differentiation and cell wall degrading enzymes in the obligately biotrophic rust fungus *Uromyces viciae-fabae*. *Botany*, 73, 624–631.
- Denoux, C., Galletti, R., Mammarella, N., Gopalan, S., Werck, D., De Lorenzo, G. et al. (2008) Activation of defense response pathways by OGs and Flg22 elicitors in *Arabidopsis* seedlings. *Molecular Plant*, 1, 423–445.
- Fan, L., Fröhlich, K., Melzer, E., Pruitt, R.N., Albert, I., Zhang, L. et al. (2022) Genotyping-by-sequencing-based identification of *Arabidopsis* pattern recognition receptor RLP32 recognizing proteobacterial translation initiation factor IF1. *Nature Communications*, 13, 1294.
- Faoro, F., Maffi, D., Cantu, D. & Iriti, M. (2008) Chemical-induced resistance against powdery mildew in barley: the effects of chitosan and benzothiadiazole. *BioControl*, 53, 387–401.
- Goldman, D.L. & Vicencio, A.G. (2012) The chitin connection. *mBio*, 3, e00056-12.
- Hao, Q., Wang, W., Han, X., Wu, J., Lyu, B., Chen, F. et al. (2018) Isochorismate-based salicylic acid biosynthesis confers basal resistance to *Fusarium graminearum* in barley. *Molecular Plant Pathology*, 19, 1995–2010.
- He, Q., Naqvi, S., McLellan, H., Boevink, P.C., Champouret, N., Hein, I. et al. (2018) Plant pathogen effector utilizes host susceptibility factor NRL1 to degrade the immune regulator SWAP70. *Proceedings of the National Academy of Sciences of the United States of America*, 115, E7834–E7843.
- Heese, A., Hann, D.R., Gimenez-Ibanez, S., Jones, A.M.E., He, K., Li, J. et al. (2007) The receptor-like kinase SERK3/BAK1 is a central regulator of innate immunity in plants. *Proceedings of the National Academy of Sciences of the United States of America*, 104, 12217–12222.
- Iriti, M., Sironi, M., Gomarasca, S., Casazza, A.P., Soave, C. & Faoro, F. (2006) Cell death-mediated antiviral effect of chitosan in tobacco. *Plant Physiology and Biochemistry*, 44, 893–900.
- Ishikawa, K., Yamaguchi, K., Sakamoto, K., Yoshimura, S., Inoue, K., Tsuge, S. et al. (2014) Bacterial effector modulation of host E3 ligase activity suppresses PAMP-triggered immunity in rice. *Nature Communications*, 5, 5430.

- Jacobs, K.A., Collins-Racie, L.A., Colbert, M., Duckett, M., Golden-Fleet, M., Kelleher, K. et al. (1997) A genetic selection for isolating cDNAs encoding secreted proteins. *Gene*, 198, 289–296.
- Jia, L.-J., Wang, W.-Q. & Tang, W.-H. (2017) Wheat coleoptile inoculation by *Fusarium graminearum* for large-scale phenotypic analysis. *Bio-Protocol*, 7, e2439.
- Jia, L.-J., Tang, H.-Y., Wang, W.-Q., Yuan, T.-L., Wei, W.-Q., Pang, B. et al. (2019) A linear nonribosomal octapeptide from *Fusarium graminearum* facilitates cell-to-cell invasion of wheat. *Nature Communications*, 10, 922.
- Jiang, C., Hei, R., Yang, Y., Zhang, S., Wang, Q., Wang, W. et al. (2020) An orphan protein of *Fusarium graminearum* modulates host immunity by mediating proteasomal degradation of TaSnRK1 α . *Nature Communications*, 11, 4382.
- Jones, J.D. & Dangl, J.L. (2006) The plant immune system. *Nature*, 444, 323–329.
- Jonkers, W., Dong, Y., Broz, K. & Kistler, H.C. (2012) The Wor1-like protein Fgp1 regulates pathogenicity, toxin synthesis and reproduction in the phytopathogenic fungus *Fusarium graminearum*. *PLoS Pathogens*, 8, e1002724.
- Kamoun, S., van West, P., Vleeshouwers, V.G.A.A., de Groot, K.E. & Govers, F. (1998) Resistance of *Nicotiana benthamiana* to *Phytophthora infestans* is mediated by the recognition of the elicitor protein INF1. *The Plant Cell*, 10, 1413–1425.
- Li, G., Zhou, J., Jia, H., Gao, Z., Fan, M., Luo, Y. et al. (2019) Mutation of a histidine-rich calcium-binding-protein gene in wheat confers resistance to Fusarium head blight. *Nature Genetics*, 51, 1106–1112.
- Liebrand, T.W.H., van den Berg, G.C.M., Zhang, Z., Smit, P., Cordewener, J.H.G., America, A.H.P. et al. (2013) Receptor-like kinase SOBIR1/EVR interacts with receptor-like proteins in plant immunity against fungal infection. *Proceedings of the National Academy of Sciences of the United States of America*, 110, 10010–10015.
- Liebrand, T.W.H., van den Burg, H.A. & Joosten, M.H.A.J. (2014) Two for all: receptor-associated kinases SOBIR1 and BAK1. *Trends in Plant Science*, 19, 123–132.
- Ma, Z., Zhu, L., Song, T., Wang, Y., Zhang, Q., Xia, Y. et al. (2017) A paralogous decoy protects *Phytophthora sojae* apoplastic effector PsXEG1 from a host inhibitor. *Science*, 355, 710–714.
- Maier, F.J., Malz, S., Löscher, A.P., Lacour, T. & Schäfer, W. (2005) Development of a highly efficient gene targeting system for *Fusarium graminearum* using the disruption of a polyketide synthase gene as a visible marker. *FEMS Yeast Research*, 5, 653–662.
- Ngou, B.P.M., Ding, P. & Jones, J.D.G. (2022) Thirty years of resistance: zig-zag through the plant immune system. *The Plant Cell*, 34, 1447–1478.
- Nie, J., Yin, Z., Li, Z., Wu, Y. & Huang, L. (2019) A small cysteine-rich protein from two kingdoms of microbes is recognized as a novel pathogen-associated molecular pattern. *New Phytologist*, 222, 995–1011.
- Nie, J., Zhou, W., Liu, J., Tan, N., Zhou, J.-M. & Huang, L. (2021) A receptor-like protein from *Nicotiana benthamiana* mediates VmE02 PAMP-triggered immunity. *New Phytologist*, 229, 2260–2272.
- Perochon, A., Kahla, A., Vranić, M., Jia, J., Malla, K.B., Craze, M. et al. (2019) A wheat NAC interacts with an orphan protein and enhances resistance to Fusarium head blight disease. *Plant Biotechnology Journal*, 17, 1892–1904.
- Piasecka, A., Jedrzejczak, N. & Bednarek, P. (2015) Secondary metabolites in plant innate immunity: conserved function of divergent chemicals. *New Phytologist*, 206, 948–964.
- Qi, M., Link, T.I., Müller, M., Hirschburger, D., Pudake, R.N., Pedley, K.F. et al. (2016) A Small cysteine-rich protein from the Asian soybean rust fungus, *Phakopsora pachyrhizi*, suppresses plant immunity. *PLoS Pathogens*, 12, e1005827.
- Qi, P.-F., Zhang, Y.-Z., Liu, C.-H., Chen, Q., Guo, Z.-R., Wang, Y. et al. (2019) Functional analysis of FgNahG clarifies the contribution of salicylic acid to wheat (*Triticum aestivum*) resistance against Fusarium head blight. *Toxins*, 11, 59.
- Seidl, M.F. & Ackerveken, G.V.D. (2019) Activity and phylogenetics of the broadly occurring family of microbial Nep1-like proteins. *Annual Review of Phytopathology*, 57, 367–386.
- Song, T., Zhang, Y., Zhang, Q., Zhang, X., Shen, D., Yu, J. et al. (2021) The N-terminus of an *Ustilagoidea virens* Ser-Thr-rich glycosylphosphatidylinositol-anchored protein elicits plant immunity as a MAMP. *Nature Communications*, 12, 2451.
- Sperschneider, J., Gardiner, D.M., Dodds, P.N., Tini, F., Covarelli, L., Singh, K.B. et al. (2016) EffectorP: predicting fungal effector proteins from secretomes using machine learning. *New Phytologist*, 210, 743–761.
- Sperschneider, J., Dodds, P.N., Singh, K.B. & Taylor, J.M. (2018) ApoplastP: prediction of effectors and plant proteins in the apoplast using machine learning. *New Phytologist*, 217, 1764–1778.
- Su, Z., Bernardo, A., Tian, B., Chen, H., Wang, S., Ma, H. et al. (2019) A deletion mutation in TaHRC confers Fhb1 resistance to Fusarium head blight in wheat. *Nature Genetics*, 51, 1099–1105.
- Van De Walle, J.V., Sergent, T., Piront, N., Toussaint, O., Schneider, Y.-J. & Larondelle, Y. (2010) Deoxynivalenol affects in vitro intestinal epithelial cell barrier integrity through inhibition of protein synthesis. *Toxicology and Applied Pharmacology*, 245, 291–298.
- Voigt, C.A., Schäfer, W. & Salomon, S. (2005) A secreted lipase of *Fusarium graminearum* is a virulence factor required for infection of cereals. *The Plant Journal*, 42, 364–375.
- Wang, L., Liu, H., Yin, Z., Li, Y., Lu, C., Wang, Q. et al. (2022) A novel guanine elicitor stimulates immunity in *Arabidopsis* and rice by ethylene and jasmonic acid signaling pathways. *Frontiers in Plant Science*, 13, 841228.
- Xu, Q., Tang, C., Wang, L., Zhao, C., Kang, Z. & Wang, X. (2020a) Haustoria – arsenals during the interaction between wheat and *Puccinia striiformis* f. sp. *tritici*. *Molecular Plant Pathology*, 21, 83–94.
- Xu, Q., Wang, J., Zhao, J., Xu, J., Sun, S., Zhang, H. et al. (2020b) A polysaccharide deacetylase from *Puccinia striiformis* f. sp. *tritici* is an important pathogenicity gene that suppresses plant immunity. *Plant Biotechnology Journal*, 18, 1830–1842.
- Yang, B., Wang, Y., Tian, M., Dai, K., Zheng, W., Liu, Z., Yang, S. et al. (2021) Fg12 ribonuclease secretion contributes to *Fusarium graminearum* virulence and induces plant cell death. *Journal of Integrative Plant Biology*, 63, 365–377.
- Zhou, X., Li, G. and Xu, J.R. (2011) Efficient approaches for generating GFP fusion and epitope-tagging constructs in filamentous fungi. *Methods in Molecular Biology*, 722, 199–212.

SUPPORTING INFORMATION

Additional supporting information can be found online in the Supporting Information section at the end of this article.

How to cite this article: Xu, Q., Hu, S., Jin, M., Xu, Y., Jiang, Q. & Ma, J. et al. (2022) The N-terminus of a *Fusarium graminearum*-secreted protein enhances broad-spectrum disease resistance in plants. *Molecular Plant Pathology*, 23, 1751–1764. Available from: <https://doi.org/10.1111/mpp.13262>